Cancer Cell
Article

SYK Is a Critical Regulator of FLT3 in Acute Myeloid Leukemia

Alexandre Puissant,[1] Nina Fenouille,[2] Gabriela Alexe,[1,3,4] Yana Pikman,[1] Christopher F. Bassil,[1] Swapnil Mehta,[1] Jinyan Du,[3] Julhash U. Kazi,[5] Frédéric Luciano,[6] Lars Rönnstrand,[5] Andrew L. Kung,[7] Jon C. Aster,[8] Ilene Galinsky,[9] Richard M. Stone,[9] Daniel J. DeAngelo,[9] Michael T. Hemann,[2] and Kimberly Stegmaier[1,3,*]

[1]Department of Pediatric Oncology, Dana-Farber Cancer Institute and Boston Children's Hospital, Harvard Medical School, Boston, MA 02215, USA
[2]Koch Institute for Integrative Cancer Research at Massachusetts Institute of Technology, Massachusetts Institute of Technology, Cambridge, MA 02139, USA
[3]The Broad Institute of Harvard University and Massachusetts Institute of Technology, Cambridge, MA 02139, USA
[4]Bioinformatics Graduate Program, Boston University, Boston, MA 02215, USA
[5]Experimental Clinical Chemistry, Department of Laboratory Medicine, Lund University, Medicon Village, 221 00 Lund, Sweden
[6]C3M/ INSERM U1065 Team Cell Death, Differentiation, Inflammation and Cancer, 06204 Nice, France
[7]Pediatric Department, Columbia University Medical Center, New York, NY 10032, USA
[8]Department of Pathology, Brigham and Women's Hospital, Harvard Medical School, Boston, MA 02215, USA
[9]Department of Medical Oncology, Dana-Farber Cancer Institute, Harvard Medical School, Boston, MA 02215, USA
*Correspondence: kimberly_stegmaier@dfci.harvard.edu
http://dx.doi.org/10.1016/j.ccr.2014.01.022

SUMMARY

Cooperative dependencies between mutant oncoproteins and wild-type proteins are critical in cancer pathogenesis and therapy resistance. Although spleen tyrosine kinase (SYK) has been implicated in hematologic malignancies, it is rarely mutated. We used kinase activity profiling to identify collaborators of SYK in acute myeloid leukemia (AML) and determined that FMS-like tyrosine kinase 3 (FLT3) is transactivated by SYK via direct binding. Highly activated SYK is predominantly found in *FLT3-ITD* positive AML and cooperates with FLT3-ITD to activate *MYC* transcriptional programs. FLT3-ITD AML cells are more vulnerable to SYK suppression than FLT3 wild-type counterparts. In a FLT3-ITD in vivo model, SYK is indispensable for myeloproliferative disease (MPD) development, and SYK overexpression promotes overt transformation to AML and resistance to FLT3-ITD-targeted therapy.

INTRODUCTION

Sequencing of acute myeloid leukemia (AML) genomes has revealed a heterogeneous disease characterized by mutations altering proliferation, differentiation programs, and the epigenetic landscape, resulting in an accumulation of immature hematopoietic cells (Ley et al., 2013). Though these mutations can result in exquisite dependency on mutant proteins, they can also lead to aberrant dependency on nonmutant proteins. For example, the histone 3 lysine 79 (H3K79) methyltransferase DOT1L has been implicated in the development of leukemias bearing translocations of the *Mixed Lineage Leukemia* (*MLL*) gene, although *DOT1L* itself is not mutated. DOT1L small-molecule inhibitors have been demonstrated in preclinical studies to selectively kill *MLL*-rearranged leukemia (Bernt et al., 2011; Daigle et al., 2011). Similarly, a small hairpin RNA (shRNA) screen targeting known chromatin regulators identified the transcriptional regulator BET bromodomain BRD4 as an epigenetic dependency in an MLL-AF9/Nras^{G12D} AML mouse model (Zuber et al., 2011). By recruiting the MLL-fusions into a transcription elongation complex, BET bromodomain proteins appear to be critical mediators for leukemogenesis involving MLL-fusion proteins (Deshpande et al., 2012).

We previously used chemical genomic, proteomic, and shRNA screening to identify SYK as a target in AML (Hahn et al., 2009). *SYK*-targeting shRNA induced AML cell differentiation in vitro,

Significance

Although imatinib therapy has been paradigm shifting for treating patients with *BCR-ABL*-rearranged chronic myelogenous leukemia (CML), the application of targeted kinase inhibitors to treating AML has been a more complex undertaking. In this study, we identified an oncogenic partnership between the most commonly mutated kinase in AML, FLT3, and the cytoplasmic kinase SYK. SYK transactivates FLT3 by a direct physical interaction, is critical for the development of FLT3-ITD-induced myeloid neoplasia, and is more highly activated in primary human FLT3-ITD-positive AML. These studies also raise the possibility of SYK activation as a mechanism of resistance to FLT3 inhibitors, suggest *FLT3* mutant AML as a subtype for SYK inhibitor testing, and nominate the clinical testing of SYK and FLT3 inhibitor combinations.

and SYK inhibition was shown to have anti-leukemia activity in AML mouse models. SYK is a cytoplasmic tyrosine kinase critical in normal B cell development and hematopoietic signaling (Mócsai et al., 2010) that was recently found to be aberrantly activated through translocations in T cell lymphoma (*ITK-SYK*) (Pechloff et al., 2010) and myelodysplastic syndrome (MDS) (*TEL-SYK*) (Kuno et al., 2001). Thus far, however, next-generation sequencing efforts have failed to identify frequent mutational events in *SYK* in AML or in B cell malignancies, where SYK dependency has also been demonstrated. In B cell malignancies, signaling from the B cell receptor (BCR) through SYK has been implicated in the pathogenesis of disease, and small molecules inhibiting SYK have had promising early clinical activity (Friedberg et al., 2010). In AML, however, little is known about the cooperative interactions of SYK in its contribution to the disease.

RESULTS

FLT3 Is a Target of SYK in AML

To identify SYK interactors in AML, we used a bead-based screening technology to profile the phosphorylation state of 80 receptor and nonreceptor tyrosine kinases, 18 tyrosine kinase signaling adaptors/regulators, and 7 tyrosine kinase signaling-linked serine/threonine kinases in the presence of activated SYK. We generated four AML cell lines stably expressing a *SYK-TEL* construct encoding a fusion protein with a constitutively active SYK kinase due to the TEL moiety that promotes homodimerization and intrinsic activation. Kinome activity in the presence of activated SYK is depicted in Figure 1A. SYK and two of its reported targets, PIK3R1 (Moon et al., 2005) and SHC1 (Umehara et al., 1998), as well as ZAP70, a member of the SYK kinase family possibly transphosphorylated by constitutively active SYK, were identified among the most hyperactivated proteins. Surprisingly, FLT3 receptor and two other platelet-derived growth factor receptor (PDGFR) family receptors, KIT and PDGFRα, also scored as top hits. Kinome activity profiling in 12 AML cell lines was next used to establish the tyrosine kinases or tyrosine kinase-regulated proteins whose activation was most highly correlated ($\rho \geq 0.5$) with basal SYK activation (Figure 1B). As in the prior screen, ZAP70, PIK3R1, and SHC1 appeared in the top correlated hits, as did FLT3 and KIT.

Our group previously demonstrated induction of myeloid differentiation in AML cells upon SYK inhibition (Hahn et al., 2009). To discover which of the PDGFR family receptors scoring in our kinase activity profiling mediates differentiation, as seen with SYK knockdown, we developed a flow-based assay to measure $CD11b^+/CD14^+$ differentiation. We transduced a panel of AML cell lines with shRNAs targeting either *SYK* or each of the identified PDGFR family kinases. Only FLT3 knockdown recapitulated the phenotypic consequence of SYK knockdown despite high knockdown efficiency in each of the kinases evaluated (Figure 1C and Figure S1 available online).

SYK Enhances FLT3 WT and Mutant Activation by Phosphorylation of Residues Y768 and Y955

Based on the kinome activity profiling results, we evaluated the phosphorylation status of the intracellular domain of the activated FLT3 receptor (GST-FLT3, 571–end) in the presence of active GST-SYK and ATP [γ-^{32}P] (Figure 2A). We found FLT3 to be directly phosphorylated by SYK, as observed by increased incorporation of γ-^{32}P.

Next, we used a phospho-mapping approach by mass spectrometry to nominate sites on the FLT3 receptor directly phosphorylated by SYK. Y726, Y768, Y842, Y899, and Y955, located in the TK1-TK2 interdomain or in the tyrosine kinase TK2 region of FLT3, were identified (Figure 2B, top). In contrast, the phosphorylation level of residue Y969, located at the extreme C-terminal region of FLT3, was not increased in the presence of SYK. In cells, a similar phospho-mapping analysis identified the same tyrosine sites to be regulated by SYK, with Y899 as the only exception (Figure 2B, bottom). These results were confirmed by an in vitro kinase assay using phosphospecific antibodies; GST-SYK increased FLT3 phosphorylation at Y768, Y842, and Y955 sites but not at site Y969 (Figure 2C). GST-SYK also promoted hyperphosphorylation of the FLT3 Y591 site, a predictor of FLT3 activity (Griffith et al., 2004).

Although this phospho-mapping approach nominated candidate FLT3 sites phosphorylated by SYK, it was not adequate to confirm direct SYK-targeted tyrosine residues because of the fact that certain FLT3 tyrosine sites, such as Y591, are also subject to autotransphosphorylation. To prevent transactivation cascades, we created a cell-based system with a kinase dead (KD; K644R) FLT3 receptor incapable of autotransphosphorylation. However, this FLT3 KD did require "prephosphorylation" to recapitulate the basal-activated state of the wild-type form of FLT3. As shown in Figures S2A and S2B, a construct encoding for V5-tagged kinase dead FLT3 [FLT3 KD (V5)] was first cotransfected with a DDK-tagged FLT3 WT (FLT3-DDK) construct to ensure the prephosphorylation of FLT3 KD (V5). The FLT3 KD (V5) was then V5-tag immunoprecipitated to separate it from the FLT3-DDK protein and incubated with GST-SYK in an in vitro kinase assay. Because FLT3 KD (V5) was now activated (phosphorylated) but unable to autotransphosphorylate, we could discriminate between sites directly phosphorylated by SYK and those autotransphosphorylated as an indirect effect of SYK-mediated FLT3 activation.

This approach was validated by V5-tag immunoprecipitation of FLT3 WT (V5) (Figure 2D). As expected, FLT3 WT was highly phosphorylated in the presence of GST-SYK. In contrast, the FLT3-KD (V5) mutant was poorly phosphorylated without prephosphorylation by FLT3-DDK. After incubation with FLT3-DDK, however, FLT3-KD (V5) was responsive to SYK phosphorylation, but because FLT3-KD (V5) was unable to autotransphosphorylate, its phosphorylation level remained lower than that of FLT3 WT (V5). This requirement for prephosphorylation of FLT3 before SYK can activate FLT3 WT (V5) further was also observed with FLT3-ITD (V5) (Figure S2C). In accordance with these results, the mutant FLT3-KD YY589/591AA, nontransphosphorylable by FLT3-DDK, was also resistant to SYK-dependent phosphorylation. We next mutated all FLT3 tyrosine residues identified by mass spectrometry into nonphosphorylatable alanines (FLT3-KD Y726A, Y768A, Y842A, Y899A, Y955A, and Y969A) to identify sites directly phosphorylated by SYK. Only two mutants, FLT3-KD (V5) Y768A and Y955A, were resistant to SYK-mediated FLT3 phosphorylation, suggesting that SYK directly phosphorylates FLT3 at sites Y768 and Y955

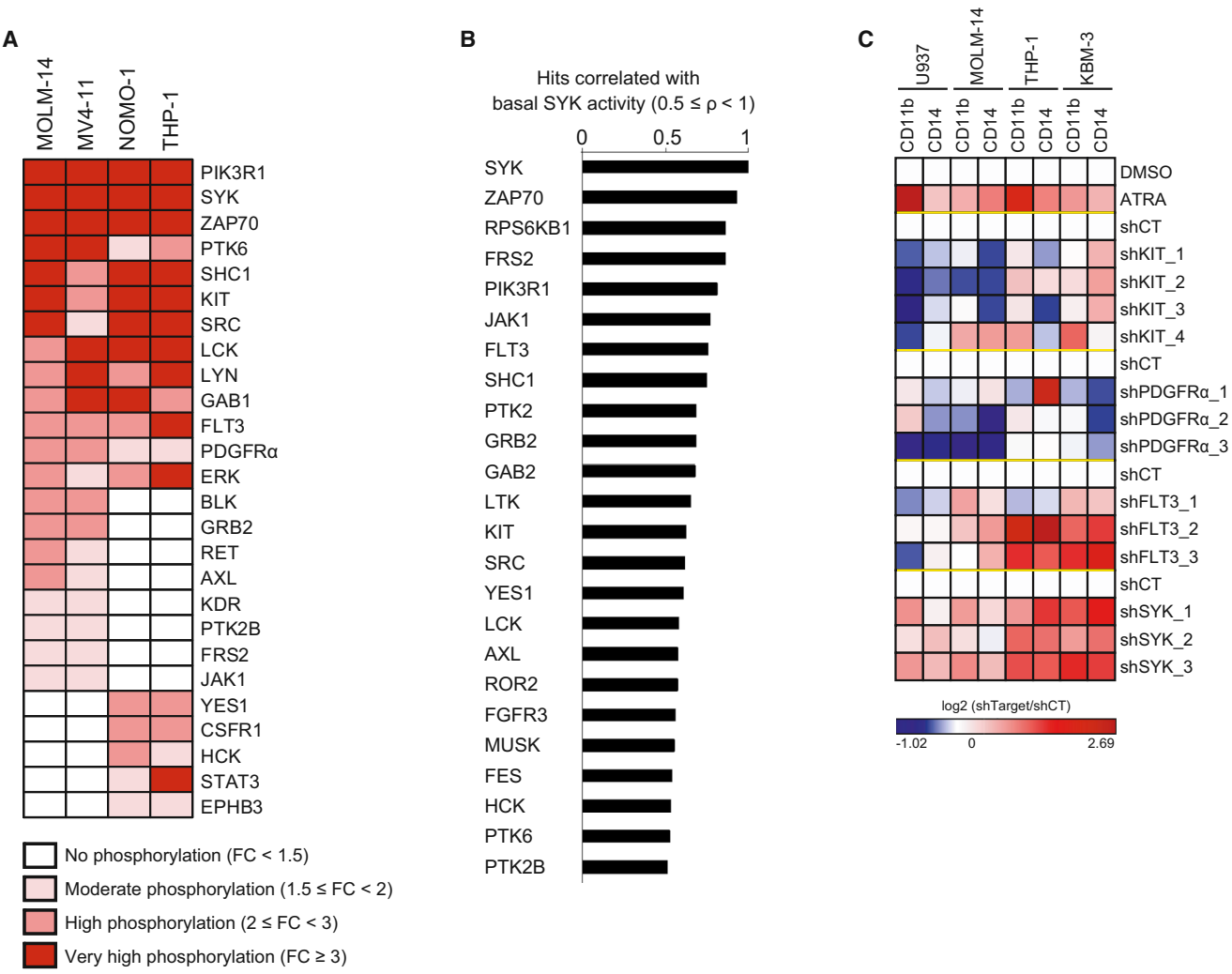

Figure 1. FLT3 Activation Correlates with SYK Activation in AML

(A) Lysates from AML cell lines stably transduced with either a constitutively activated form of SYK (SYK-TEL) or an empty vector (CT) were evaluated by kinase activity profiling. The log_2-transformed ratio (SYK-TEL versus CT) of tyrosine phosphorylation is depicted as a heatmap where each protein is ranked by its phosphorylation level across the cell lines. FC, fold change.

(B) Spearman correlation between basal phosphorylation of SYK compared to all other detected candidates in the kinase activity profiling assay across 12 AML cell lines. The most highly correlated hits ($\rho \geq 0.5$) are represented on the histogram.

(C) Heatmap showing level of CD14 and CD11b-positive myeloid differentiation in AML cell lines treated with ATRA or transduced with a control shRNA (shCT) or *KIT*-, *PDGFRα*-, *FLT3*-, or *SYK*-targeting shRNAs. Normalized data are presented as a log_2-ratio (shTarget versus shCT).

See also Figure S1.

(Figure 2D). These two mutations completely abrogated SYK-mediated FLT3 activation, with a consequent downregulation of FLT3 activation at site Y591 (Figure 2E).

FLT3 mutations are the most common genetic alterations in AML. Internal tandem duplication (ITD) mutations within the FLT3 juxtamembrane domain occur in 20%–30%, and other point mutations (i.e., D835Y or D835V) in the tyrosine-kinase domain (FLT3-TKD) occur in an additional 7%–9% of AML (Swords et al., 2012). By an in vitro kinase assay, we determined that the well-described *FLT3* mutants *FLT3-ITD* and D835Y were also SYK phosphorylated (Figure 2F). WT and mutant FLT3 showed increased SYK phosphorylation at Y768 and Y955, which is strongly associated with increased FLT3 activation at Y591 as well as activation of known FLT3 targets STAT5 and ERK1/2 (Figure 2G). Of note, overexpression of inactive SYK KD induced neither FLT3 phosphorylation nor the activation of ERK1/2.

FLT3 Activation by SYK Depends on a Physical Interaction

We used two approaches to investigate the effects of SYK on FLT3 activation in a cellular context. First, using recently generated small-molecule inhibitors of SYK, PRT062607 (Spurgeon et al., 2013) and Merck SYKi (Moy et al., 2013), we determined both in AML cell lines and primary patient samples that SYK inhibition diminished FLT3 activation in a few hours, as reflected

by the downregulation of FLT3 phosphorylation at site Y591 and at the SYK-phosphorylated sites Y768 and Y955. This was accompanied by an inhibition of downstream STAT5 and ERK1/2 signaling (Figures 3A, 3B and S3A). Next, to confirm that this effect was on target for SYK, we used a doxycycline-inducible microRNA (miRNA)-based short hairpin RNA (miR30-shRNA) system to produce knockdown approximating that of a null allele. Expression of two different miR30-shRNAs targeting *SYK* (shSYK_4 and shSYK_5) induced a time-dependent downregulation of SYK expression, loss of FLT3 phosphorylation at Y768, Y955, and Y591, and a decrease in STAT5 activation (Figure 3C).

To further validate these results, we overexpressed a constitutively activated SYK (*SYK-TEL*) to assess its effects on FLT3 activation and its downstream effectors (Figure S3B). We also generated a *TEL-SYK* chimera, a fusion between a truncated form of *SYK* lacking its SH2 domains (SH2 Nter + SH2 Cter) and a *TEL* sequence substituting for these SH2 domains (Kuno et al., 2001). Transduction of wild-type *SYK* (SYK WT) into two AML cell lines with low basal levels of SYK activation, THP-1 and NOMO-1, enabled expression of moderately activated SYK, whereas the *SYK-TEL* construct encoded for a highly activated form (Figure 3D). When these two constructs were expressed, FLT3 phosphorylation at Y768 and Y955 increased, and FLT3 activation was enhanced, as demonstrated by Y591 phosphorylation and hyperactivation of the downstream STAT5, AKT, and ERK1/2 pathways. FLT3 phosphorylation was even more pronounced with *SYK-TEL* than *SYK* WT expression, an effect that was abrogated in the presence of KD (K402R) mutants. These results were confirmed in 293E cells transfected with *SYK* WT and *SYK-TEL* constructs. Surprisingly, however, *TEL-SYK*, which, like *SYK-TEL*, enabled overexpression of a constitutive active SYK, did not fully recapitulate the effects of *SYK-TEL* on FLT3 activation (Figure 3E).

We thus hypothesized that the SH2-binding region expressed on SYK-TEL but absent on TEL-SYK supports an essential interaction between SYK and FLT3 needed for phosphorylation of FLT3 by SYK. To test this, we coexpressed V5-tagged FLT3 WT with either SYK WT or the chimeric proteins TEL-SYK and SYK-TEL WT or KD in 293E cells (Figure 3F). We determined that the SYK WT, SYK-TEL WT, and KD expressed proteins, along with a SYK mutant (Y130E) reported to be activated in the presence of BCR (Keshvara et al., 1997), coimmunoprecipitated with FLT3, whereas the TEL-SYK fusion protein did not. However, as confirmed in Figure S3C, the TEL moiety did not markedly alter the binding capacity to FLT3 WT or mutant. To confirm that SYK interacted with FLT3 through its SH2-binding region, we generated several SYK mutants by deleting the SH2 N-terminal, C-terminal, or both domains (ΔSH2 Nter, ΔSH2 Cter, and ΔSH2 Nter + Cter) or by inactivation of these domains by point mutation (SH2 Nter$^{mut\ (42RQS\ >\ GGI)}$, SH2 Cter$^{mut\ (195RAR\ >\ GAL)}$ and SH2 Nter + Cter^{mut}) (Figure 3G). Only SYK mutants lacking the SH2 Cter domain or mutated in the SH2 Cter domain failed to coimmunoprecipitate with FLT3, demonstrating that the SYK SH2 C-terminal domain is involved in FLT3 binding. Notably, cytoplasmic sequestration of a SYK mutant with deletion of the nuclear localization sequence (SYK ΔNLS) enhanced the association of that mutant with FLT3. Mutagenesis of *FLT3* revealed a tetrad of tyrosine residues Y589, Y591, Y597, and Y599 located in the juxtamembrane region of FLT3 as essential for this physical interaction (Figures S3D and S3E). To see if SYK interacted more avidly with FLT3-ITD than WT, we immunoprecipitated SYK in cells expressing isogenic pairs of FLT3 constructs. As observed in Figure 3H, SYK showed greater affinity for FLT3-ITD than FLT3 WT. Finally, we validated the endogenous interaction between SYK and FLT3 in a panel of 12 AML cell lines expressing various levels of either FLT3 WT or ITD (Figure 3I). A fraction of SYK associated with FLT3 is activated, as shown by phosphorylation of SYK at Y525/Y526. Using confocal microscopy on primary AML patient samples, we identified that the proteins interacted predominantly at the cellular membrane, suggesting that FLT3 (APC) trapped SYK (FITC) at FLT3′s primary site of localization (Figure 3J).

SYK Is Required for FLT3-ITD-Induced Myeloid Disease

We next investigated whether SYK was required for FLT3-ITD-dependent myeloproliferative disease (MPD). We used miR30-shRNA to stably and efficiently knockdown *Sykb* (homologous to human *SYK*) in murine myeloid progenitors. As depicted in Figure 4A, murine myeloid progenitors (common myeloid progenitor [CMP] and granulocyte/monocyte progenitor [GMP] cells) expressed high levels of *Sykb* compared to more immature LSK cells. The Sca-1^{-}/c-KIT^{+} myeloid progenitor fraction from donor mice whole bone marrow was transduced first with one nontargeting control (CT) miR30-shRNA or the two most effective hairpins directed against *Sykb* (miR30-shSykb1 and miR30-shSykb4) before sorting and transduction with the MSCV-EGFP empty (MIG) or *FLT3-ITD* vector (Figure S4A). Transduction efficiency was analyzed by flow cytometry to confirm that GFP expression occurred only in the tomato-positive cell fraction (Figure S4B) and knockdown confirmed by western blot (Figure S4C).

Animals receiving miR30-shCT + *FLT3-ITD* developed marked splenomegaly, with spleens two to seven times larger than those of the miR30-shCT + MIG mice (Figure 4B). These mice also developed a striking leukocytosis and an approximately 2-fold decrease in both hematocrit (HCT) and platelet (PLT) count compared to miR30-shCT + MIG-transplanted mice, an effect abrogated with Sykb knockdown (Figures 4B and S4D). Similarly, miR30-shCT + *FLT3-ITD* mice developed a lethal hematopoietic disease with a median latency of approximately 75 days, whereas animals transplanted with *FLT3-ITD* and either miR30-shSykb1 or miR30-shSykb4 cells exhibited almost normal overall survival at 150-day follow up (Figure 4C).

In *FLT3-ITD* + miR30-shCT spleen and blood, flow cytometric analysis showed a marked increase in cells positive for the late myeloid markers GR-1 and Mac-1, respectively, indicative of granulocytes (GR-1^{+}/Mac-1^{+}) and monocytes (GR-1^{-}/Mac-1^{+}), compared to the spleen and blood cells of control mice (Figure 4D). The majority of these mature myeloid cells were both tomato and GFP positive, demonstrating that they arose from *FLT3-ITD* + miR30-shCT-transduced marrow. In contrast, the *Sykb*-depleted *FLT3-ITD* mice displayed a minimal increase in granulocytes in blood and spleen, largely tomato and GFP negative. Finally, *FLT3-ITD*-mediated myeloid expansion was accompanied by a reduction in lymphoid maturation, as assessed by a decrease in the number of B220 or CD3-positive

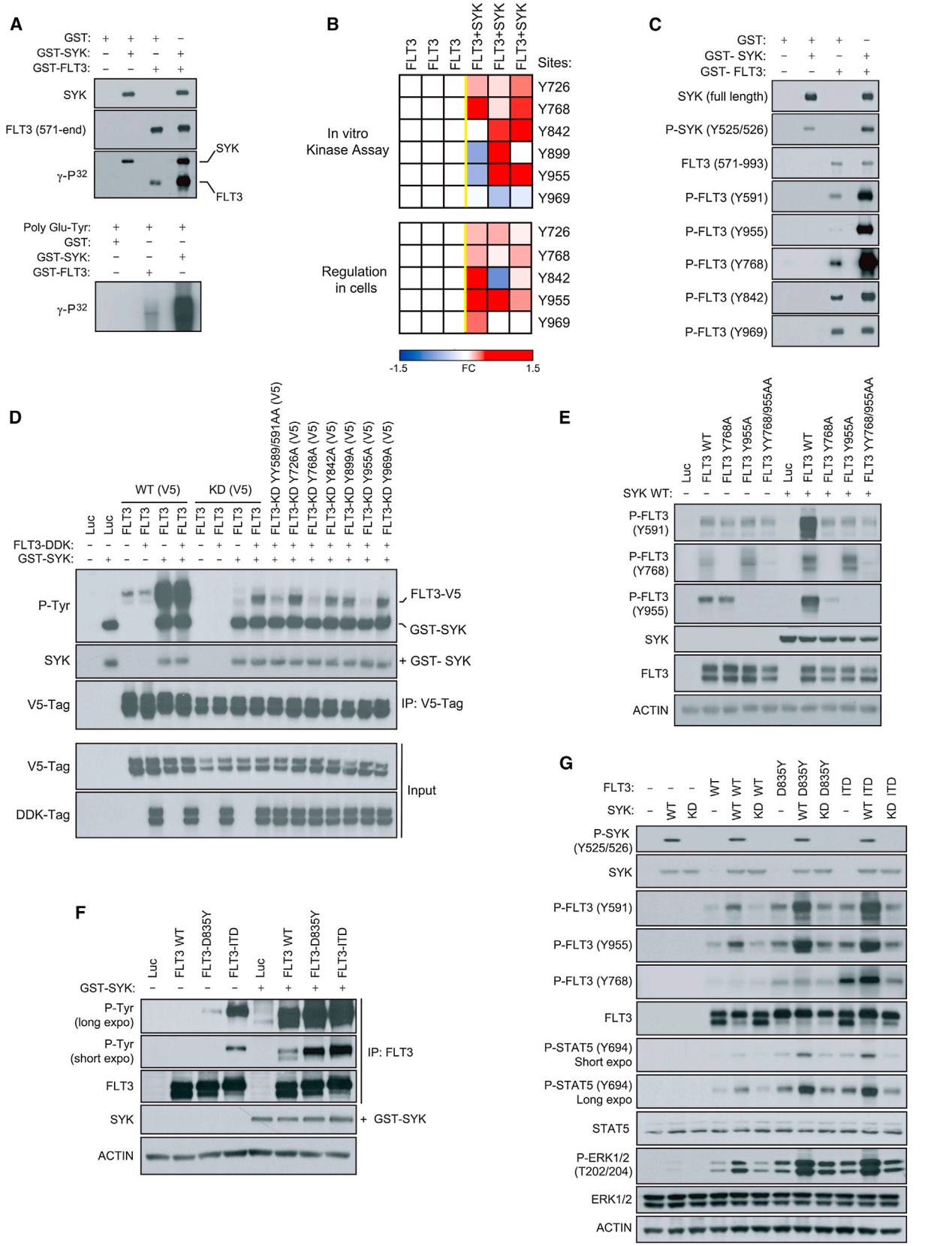

(legend on next page)

cells in spleen and blood from *FLT3-ITD* + shCT mice. As expected, *Sykb* knockdown restored a normal proportion of these lymphoid cells (Figure S4E).

Finally, we detected by fragment analyzer the presence of *FLT3-ITD* sequence in genomic DNA extracted from bone marrow and spleen cells to ensure stable insertion of the mutation (Figure S4F). Although the *FLT3-ITD* sequence was highly represented in the bone marrow and spleen of mice transplanted with miR30-shCT infected cells, its abundance was strongly decreased in *Sykb*-depleted counterparts, suggesting suppression of *FLT3-ITD* positive cells.

To rule out the possibility that this phenotype resulted from failed engraftment of *FLT3-ITD*-positive cells, we used a complementary approach: doxycycline-induction of *Sykb* knockdown in murine myeloid cells already transformed by *FLT3-ITD* (Figure S4G). From the TRMPVIR doxycycline-inducible vector, we engineered a TRMPCIR vector by substitution of the yellow-green Venus reporter for a far-red fluorescent Crimson sequence suitable for cotransduction with the *FLT3-ITD* GFP vector (Figure S4H). Transduction efficiency was analyzed by flow cytometry to confirm that GFP expression occurred only in crimson-positive cells (Figure S4I). The normalization of the white blood cell (WBC) count and a marked decrease in FLT3-ITD-positive cells were observed following induction of *Sykb* knockdown at the onset of disease, an effect sustained after doxycycline withdrawal (Figures 4E and 4F). This resulted in a significant improvement in the overall survival of *FLT3-ITD* + miR30-shSykb1 and *FLT3-ITD* + miR30-shSykb4 mice in comparison to *FLT3-ITD* + miR30-shCT mice (Figure 4G). In vitro, we confirmed that doxycycline-induced suppression of *Sykb* decreased FLT3 activity at Y591 and profoundly altered growth of the *FLT3-ITD*-transduced myeloid cells from 5 to 12 days after doxycycline (Figures 4H and 4I). Finally, to investigate whether FLT3-ITD AML cells are more vulnerable to SYK inhibition than FLT3 WT AML, we screened several genetically defined AML cell lines (Figures 4J and 4K) and patient AML samples (Figures 4L and 4M) for sensitivity to doxycycline-mediated SYK knockdown or SYK-specific inhibitors PRT062607 and Merck SYKi. FLT3-ITD positive AML cell lines and patient primary cells were strikingly more sensitive to SYK targeting by shRNA or small-molecule inhibitors than were their FLT3 WT counterparts (Figures 4J–4M).

Highly Activated SYK Cooperates with FLT3-ITD in Primary Patient AML

To assess the representation of highly versus minimally activated SYK across cohorts of patient samples, we profiled three AML cell lines transduced with either control or *SYK*-targeting shRNAs using genome-wide transcriptional profiling. SYK knockdown prompted a dynamic change in transcription, with 115 genes significantly upregulated and 95 genes significantly downregulated based on permutation $p < 0.05$ and FDR < 0.05 for signal-to-noise ratio (SNR). The top differentially 45 upregulated and 36 downregulated genes are depicted in Figure 5A. The full list is reported in Table S1. As expected, SYK expression was significantly downregulated across all AML cell lines in response to the two *SYK*-targeting shRNAs (Figure S5A). Next, we used this complete SYK gene set (Table S1) to query by single sample gene set enrichment analysis (ssGSEA) three cohorts of AML patient samples (GSE14468, GSE10358, and TCGA LAML), revealing that patients with a SYK-high signature were predominantly present in French-American-British (FAB) classification M1, whereas FAB M4 AML was enriched in patients with the SYK-low signature (Figure S5B). An analogous investigation applied to the two largest cohorts of FLT3-ITD AMLs, GSE14468 and TCGA LAML, showed that the SYK-high signature frequency is significantly higher in the *ITD* mutant than in the wild-type *FLT3* subgroup (Figure 5B). An extension of this analysis to other known mutations in AML (*NPM1*, *DNMT3A*, *IDH1/2*, *RUNX1*, *TET2*, *TP53*, *KRAS*, *NRAS*, *CEBPA*, *WT1*, and *KIT*; data not shown) revealed no significant positive correlation between the SYK-high signature and any of these mutations. However, in the GSE14468 and GSE10358 cohorts, the frequency of patients with the SYK-low signature is higher in *NPM1* mutants than in the wild-type *NPM1* subgroup. This trend was also observed in patients with double *FLT3-ITD* and *NPM1* mutations (Figure S5C).

We then used a complementary flow cytometry approach to assess an independent group of primary patient AML samples with either wild-type *FLT3* (n = 25) or *FLT3-ITD* (n = 23) for SYK and FLT3 activation levels using P-SYK (Y525/526) or P-FLT3 (Y591) directed antibodies (Figures 5C and 5D). As observed when using SYK transcriptional signatures as surrogates for SYK activation, primary patient AML samples with high P-SYK levels appeared more frequently in the *ITD* than in the wild-type

Figure 2. SYK Phosphorylates FLT3 WT and Mutants at Sites Y768 and Y955

(A) In vitro kinase assay showing incorporation of γ-^{32}P in response to the incubation of active GST-FLT3 (571–end) with active GST-SYK. The poly Glu-Tyr universal substrate peptide is used to validate FLT3 and SYK kinase activity.

(B) FLT3 phosphorylation state from an in vitro kinase assay performed with active GST-SYK (top) or immunoprecipitated from 293E cells transfected with FLT3-V5 and SYK WT (bottom) was analyzed by targeted mass spectrometry and phosphorylation ratios determined from chromatographic peak intensities. Heatmap showing the level of tyrosine phosphorylation of three biological replicates. Fold change (FC) is presented as a $\log_2$ ratio [exp(FLT3+SYK)/exp(FLT3)].

(C) In vitro kinase assay performed by incubating active GST-FLT3 (571–end) with active GST-SYK and immunoblotted using phosphospecific FLT3 and SYK antibodies.

(D) V5-tagged *FLT3* WT [*FLT3* WT (V5)] or kinase dead [*FLT3*-KD (V5)] with tyrosines either wild-type or mutated to alanine were cotransfected into 293E cells along with a DDK-tagged *FLT3* WT (*FLT3*-DDK) vector. V5-tagged constructs were then V5-tag immunoprecipitated to purify out the FLT3-DDK protein before incubation with GST-SYK for an in vitro kinase assay. Global FLT3 phosphorylation level was detected by immunoblot using an anti-phospho-tyrosine (P-Tyr) antibody.

(E) Western blot for FLT3 specific phosphosites from 293E cells coexpressing FLT3 WT or FLT3 Y768A, Y955A and YY768/955AA mutants, and SYK WT.

(F) FLT3 WT, D835Y, and ITD immunoprecipitated from 293E cells expressing each of these constructs and incubated with GST-SYK for an in vitro kinase assay. Detection of global FLT3 phosphorylation level using anti-phospho-tyrosine (P-Tyr) antibody.

(G) Western blot for FLT3 specific phosphosites from 293E cells coexpressing FLT3 WT, D835Y or ITD, and SYK WT or kinase dead (KD).

See also Figure S2.

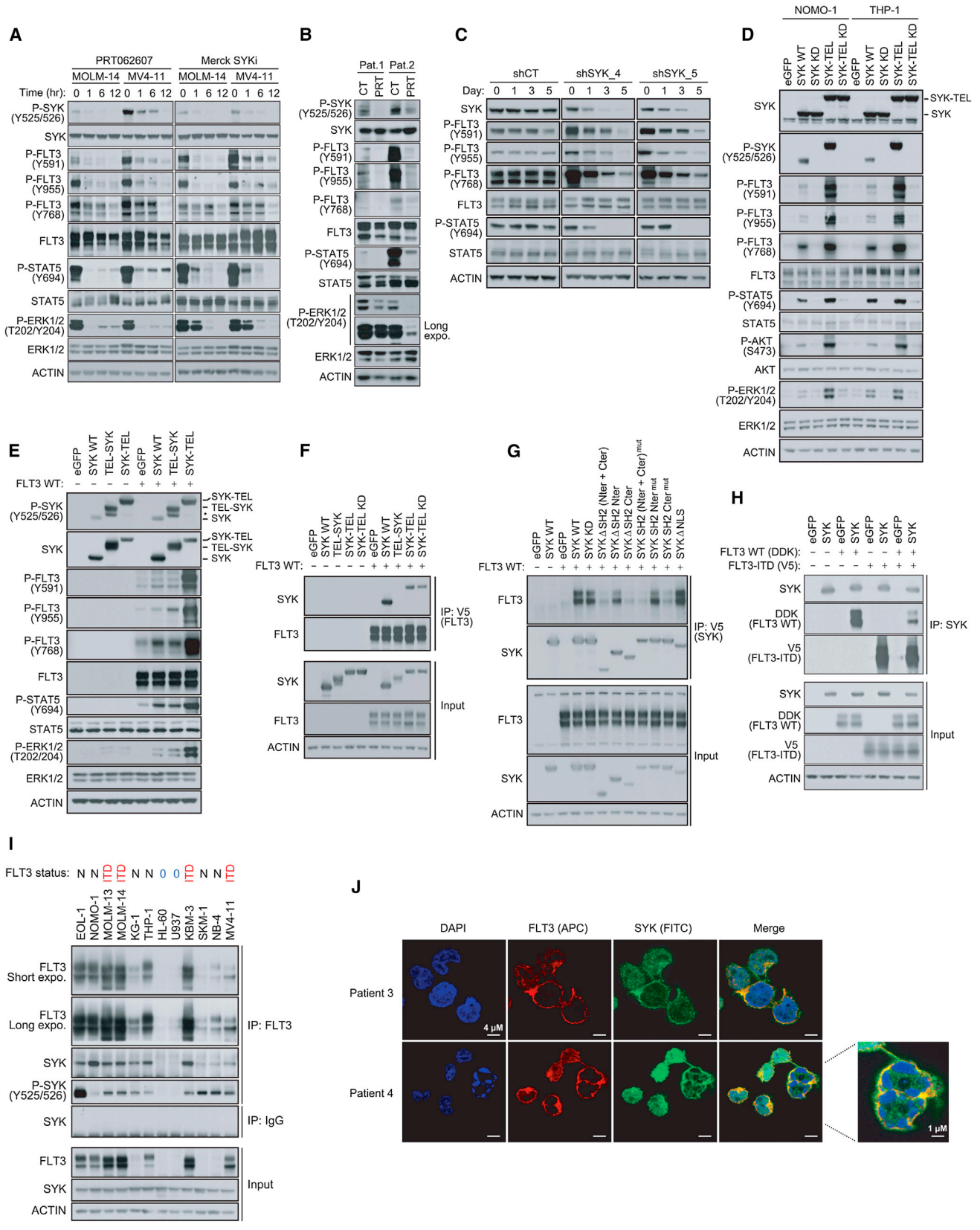

(legend on next page)

FLT3 subgroup (Figure 5C). To further characterize this association, each subgroup of patients was scaled on X-Y graphs based on their P-SYK/SYK and P-FLT3/FLT3 *Z* scores (Figures 5D and S5D). As expected, FLT3 was more highly activated in patients with *FLT3-ITD*, and P-SYK and P-FLT3 activation levels were more strikingly correlated in patients with *FLT3-ITD* (ρ score = 0.7) than with wild-type *FLT3* (ρ score = 0.5). Interestingly, SYK and FLT3 activation were most highly correlated in patients with relapsed AML expressing the *FLT3-ITD* mutation (ρ score = 0.8).

We divided FLT3-ITD patient samples from three AML data sets into two groups based on SYK signature (high versus low) and interrogated the data with published, validated gene signatures (available from Molecular Signature Data Base [MSig] and Differentiation Map [DMAP]) for enrichment by ssGSEA. As shown in Figures 5E and S5E and Tables S2 and S3, gene sets associated with hematopoietic progenitor maintenance and MYC-dependent transcriptional programs were significantly enriched in the FLT3-ITD samples displaying a high SYK signature and depleted in those displaying a low SYK signature. High P-SYK activation combined with FLT3-ITD mutation is associated with overexpression of MYC at both mRNA and protein levels (Figures 5F and 5G). Finally, using top genes from human and murine MYC target-related gene sets, we designed a MYC consensus transcriptional target mini signature. We used quantitative RT-PCR (qRT-PCR) to assess alteration of these signature genes in Ba/F3 or U937 cells coexpressing FLT3-ITD and SYK or SYK-TEL constructs (Figure 5H). These results suggest that a pro-leukemogenic, cooperative interaction between FLT3-ITD and SYK may select for higher levels of SYK activation in FLT3-driven disease and that SYK may promote MYC expression and activation as a mechanism of leukemogenesis.

SYK Activation Promotes Progression of FLT3-ITD-MPD to AML

We generated a second bone marrow transplantation model using sorted myeloid progenitors cotransduced with MSCV-EGFP-FLT3-ITD in combination with MSCV-tomato vectors (MIT) encoding for either wild-type SYK (SYK WT), a constitutively activated SYK-TEL, or TEL-SYK (Figure S6A). Before re-injection, transduction efficiency was analyzed by flow cytometry to confirm that GFP expression occurred in the tomato-positive cell fraction (Figure S6B).

Although mice that received myeloid cells cotransduced with *FLT3-ITD* and MIT developed a lethal disease (median latency 73 days) (Figure 6A), mice transplanted with cells expressing *FLT3-ITD* and either *SYK* or *SYK-TEL* constructs developed a disease with a more rapid onset and a reduced median latency (64 and 43 days, respectively) (Figure 6A). However, animals injected with cells expressing both *FLT3-ITD* and *TEL-SYK* constructs did not show signs of more accelerated disease, suggesting that both the level of SYK activation and the capacity for binding and transactivation of FLT3 are essential to modulate FLT3-ITD disease progression. Importantly, groups receiving *SYK-TEL*- or *TEL-SYK*-expressing cells contracted a lethal disease by 180 days posttransplantation, as compared to control mice showing no lethality for up to 220 days (data not shown).

The decreased overall survival of mice injected with cells coexpressing either *SYK* or *SYK-TEL* and *FLT3-ITD* was associated with marked splenomegaly, as compared to mice transduced only with *FLT3-ITD* (Figure 6B). These mice also exhibited elevated WBC counts, anemia, and thrombocytopenia (Figure S6C). *FLT3-ITD* sequence levels were more elevated in spleens of mice coexpressing *SYK* and *SYK-TEL* based on fragment analyzer (Figure S6D). In addition, qRT-PCR using primers specific for a common region of *SYK*, *SYK-TEL*, and *TEL-SYK* confirmed homogeneous expression of each construct on an equivalent number of infected spleen-sorted cells (Figure S6E).

Consistent with the myeloproliferative phenotype described earlier, an increase in a myeloid cell population positive for GR-1 and Mac-1 was observed in spleen cells from *FLT3-ITD* + MIT mice compared to those from control MIT + MIG mice (Figure 6C). However, this cell fraction was more highly represented in the spleens of mice transplanted with either *SYK* or *SYK-TEL* constructs combined with *FLT3-ITD* than in those injected with cells coexpressing *TEL-SYK* and *FLT3-ITD*. H&E staining of *FLT3-ITD* + MIT spleen and bone marrow showed a marked predominance of maturing myeloid lineage cells, consistent with MPD, whereas spleens and bone marrow harvested from mice expressing either *SYK* or *SYK-TEL* constructs combined with *FLT3-ITD* showed extensive infiltration

Figure 3. Activation of FLT3 and Its Downstream Effectors Is Dependent on a Physical Interaction with SYK.

(A) Western blot for indicated proteins from MOLM-14 and MV4-11 cells treated with 3 μM PRT062607 or 5 μM Merck SYKi. The phosphosite Y768 was detected on FLT3 total immunoprecipitate.

(B) Western blot for indicated proteins from FLT3-ITD positive primary patient AML cells treated for 6 hr with 3 μM PRT062607.

(C) Western blot for SYK and FLT3 specific phosphosites from MOLM-14 cells stably transduced with either a control or two *SYK*-targeting doxycycline-inducible miR30-shRNAs and treated with doxycycline for 1, 3, or 5 days. The phosphosite Y768 was detected on FLT3 total immunoprecipitate.

(D) Western blot for indicated proteins from NOMO-1 and THP-1 AML cells expressing different forms of SYK. The phosphosite Y768 was detected on FLT3 total immunoprecipitate.

(E) Western blot for FLT3, STAT5, and ERK specific phosphosites from 293E cells expressing FLT3 WT and different forms of SYK.

(F) Using anti-V5 antibody, FLT3 immunoprecipitation from 293E cells coexpressing FLT3 and different forms of untagged SYK and western blot using anti-SYK antibody.

(G) Using anti-V5 antibody, immunoprecipitation of several truncated and mutated forms of SYK from 293E cells coexpressing these constructs and untagged FLT3 WT and western blot using anti-FLT3 antibody.

(H) Using anti-SYK antibody, immunoprecipitation of SYK from 293E cells coexpressing isogenic pairs of FLT3 WT and ITD constructs and western blot using anti-SYK, anti-V5, and anti-DDK antibodies.

(I) FLT3 immunoprecipitation from 12 AML cell lines expressing low levels of FLT3 WT (0) and various levels of FLT3 WT (N) or mutated (ITD) and western blot using anti-SYK and anti-P-SYK (Y525/526) antibodies. Anti-IgG antibody was used as a control.

(J) Staining for SYK (green), FLT3 (red), and DAPI (blue) in blast cells from two FLT3-ITD positive primary patient AML samples.

See also Figure S3.

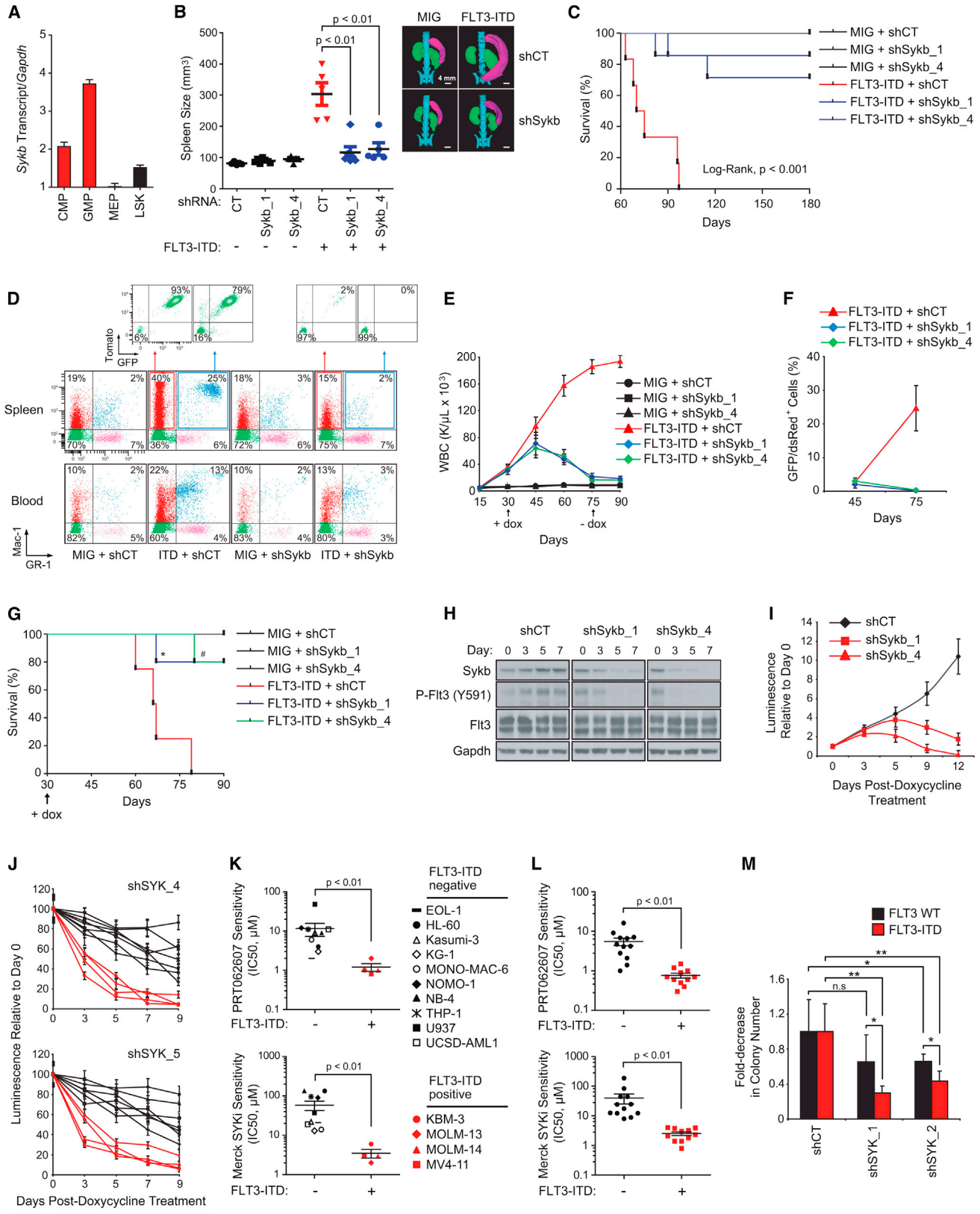

(legend on next page)

by sheets of immature myeloid blasts, consistent with AML, in about 65% to 75% of cases, respectively (Figure 6D). Furthermore, a population of tomato- and GFP-positive cells positive for the hematopoietic progenitor marker c-KIT was also found in spleens from all *FLT3-ITD* + *SYK* and *FLT3-ITD* + *SYK-TEL* moribund animals, but not in spleens of other *FLT3-ITD* groups (Figure 6E). These results suggest that the MPD observed with *FLT3-ITD* alone has a more immature phenotype when *FLT3-ITD* is combined with *SYK* or *SYK-TEL* activation consistent with AML.

Several FLT3-ITD + SYK or SYK-TEL moribund animals showed a recurrent expansion of the Lin^{Low}/Sca-1^{-}/c-KIT^{+}/$CD16/32^{+}$/$CD34^{+}$ GMP compartment (n = 5/7 and n = 4/6, respectively; representative examples in Figure 6F). Whereas FLT3-ITD alone enhanced the expansion of the GMP population by 1.5-fold, the proportion of GMP cells expressing either *FLT3-ITD* + *SYK* or *FLT3-ITD* + *SYK-TEL* was increased by 2.5- and 4.5-fold, respectively. Simultaneous expression of *FLT3-ITD* and either *SYK* or *SYK-TEL* results in a growth advantage of this fraction at the expense of megakaryocyte/erythrocyte progenitor (MEP) and CMP fractions, because, in both cases, double tomato/GFP-positive GMP clones emerged from the whole GMP population. Finally, *SYK* and, even more dramatically, *SYK-TEL* expression enhanced the growth capacity of *FLT3-ITD*-expressing $tomato^{+}$/GFP^{+} myeloid cells in vitro over 9 days (Figure 6G). We also assessed the effect of SYK and FLT3-ITD cooperation on the clonogenic potential of normal purified $CD34^{+}$ human cells. As shown in Figure 6H, the number of $CD34^{+}$ colonies significantly increased with cotransduction of *FLT3-ITD* and either *SYK* WT or *SYK-TEL* in comparison to FLT3-ITD only controls. This increase relies on SYK activity, because it was not observed in the presence of the KD mutant of SYK-TEL (SYK-TEL KD). Further mutation of FLT3-ITD's SYK phosphorylation sites, Y768 and Y955, into alanines undermined the cooperation of SYK with FLT3-ITD in promoting colony formation (Figure 6I). An analogous experiment was conducted in vivo (Figure 6J). Unfortunately, YY768/955AA and Y768A mutants impeded *FLT3-ITD*'s ability to induce a lethal MPD. However, although the FLT3-ITD Y955 mutant generated a low-penetrance lethal disease, it did block acceleration of the disease induced by SYK-TEL coexpression.

To determine the degree to which a potentially promiscuous kinase such as SYK would have a similar effect on other mutated tyrosine kinase oncogenes, we evaluated a BCR-ABL-driven leukemia model. By kinome profiling and in vitro kinase assay, we determined that ABL was neither an indirect nor a direct target of SYK (data not shown and Figure S6F). We used an acute lymphocytic leukemia model of murine $p19^{Arf\ -/-}$ pre-B cells driven by *Bcr-Abl* transplantable into immune-competent syngeneic C57/BL6 mice (Williams et al., 2006). As shown in Figures S6G and S6H, SYK-TEL overexpression neither amplified growth of BCR-ABL-positive cells in bone marrow or spleen nor influenced survival. Furthermore, SYK-TEL overexpression did not significantly enhance the number of colonies of either $CD34^{+}$ cells transduced with BCR-ABL or CD34+ BCR-ABL positive cells purified from a patient with chronic myeloid leukemia (CML) (Figures S6I and S6J). These results suggest that activated SYK does not exert the same pro-oncogenic effect on other tyrosine kinase oncogenes, such as BCR-ABL, as it does on FLT3-ITD.

SYK Activation Promotes Resistance to Targeted Kinase Inhibitors

We next asked whether the *FLT3-ITD/SYK* models could be transplanted into secondary recipients. $Tomato^{+}$/GFP^{+} myeloid cells expressing *FLT3-ITD* in combination with MIT empty, *SYK* WT, or *SYK-TEL* were sorted from spleens of moribund donor mice and reinjected into sublethally irradiated recipient mice. Although FLT3-ITD + MIT-expressing cells did not alter mice survival, purified FLT3-ITD + SYK or SYK-TEL cells generated a lethal disease in secondary recipients with median latencies of 64 and 19–28 days, respectively (Figure 7A) and induced previously observed features, including increased WBC, decreased PLT count and HCT, and marked splenomegaly (Figures

Figure 4. SYK Knockdown Impairs Development of FLT3-ITD-Driven Myeloid Disease

(A) qRT-PCR showing relative expression levels of *Sykb* in purified progenitor hematopoietic stem and progenitor subsets. Error bars represent mean ± SD.

(B) Spleen size measurement by microtomography of five mice per group. One representative picture is shown for one mouse per indicated group. $p < 0.01$ calculated using a Mann-Whitney test. Error bars represent mean ± SEM.

(C) Kaplan-Meier curves showing overall survival of mice (n = 6) transplanted with myeloid cells expressing each combination of MSCV and miR30-shRNA vectors. Statistical significance determined by log-rank (Mantel-Cox) test.

(D) FACS analysis of Mac-1 and GR-1 expressing populations in spleen and blood. A representative FACS plot from each group is shown.

(E) WBC count in the blood harvested from three mice per group. The p value was calculated using a Mann-Whitney test. Arrow indicates beginning and end of doxycycline treatment. Error bars represent mean ± SEM.

(F) FACS analysis of GFP/dsRed-positive cells in bone marrow with error bars representing the mean ± SEM of three bleedings per time point.

(G) Kaplan-Meier curves showing overall survival of mice (n = 4 for MIG and FLT3-ITD + shCT groups; n = 6 for FLT3-ITD + shSykb groups) transplanted with myeloid cells expressing each combination of MSCV and doxycycline-inducible vectors (TRMPCIR). Statistical significance determined by log-rank (Mantel-Cox) test. $^{*}p = 0.02$ and $^{\#}p = 0.003$ by comparison with FLT3-ITD + shCT group. Arrow indicates beginning of doxycycline treatment.

(H) Western blot indicating the expression level of SYK and FLT3 activity over 7 days after doxycycline.

(I) Growth after treatment with doxycycline is shown relative to day 0 (time of seeding), with error bars representing the mean ± SD.

(J) AML cell lines were infected with two *SYK*-directed shRNAs. Growth after doxycycline is normalized to the control shRNA and shown relative to day 0 (time of seeding), with error bars representing the mean ± SD.

(K and L) Distribution of IC_{50} for *FLT3* wild-type versus *FLT3-ITD* AML cell lines (K) or patient primary cells (L) in response to treatment with PRT062607 or Merck SYKi. The p value was calculated using nonparametric Mann-Whitney test.

(M) $CD34^{+}$ primary cells from *FLT3* WT (n = 4) or *ITD* (n = 5) patients with AML were purified and infected with shCT or two *SYK*-targeting shRNAs. Colony number was evaluated after MTT staining. $^{**}p < 0.01$, $^{*}p \leq 0.05$ calculated using a Mann-Whitney test. n.s, non significant ($p > 0.05$).

Error bars represent mean ± SEM (K–M).

See also Figure S4.

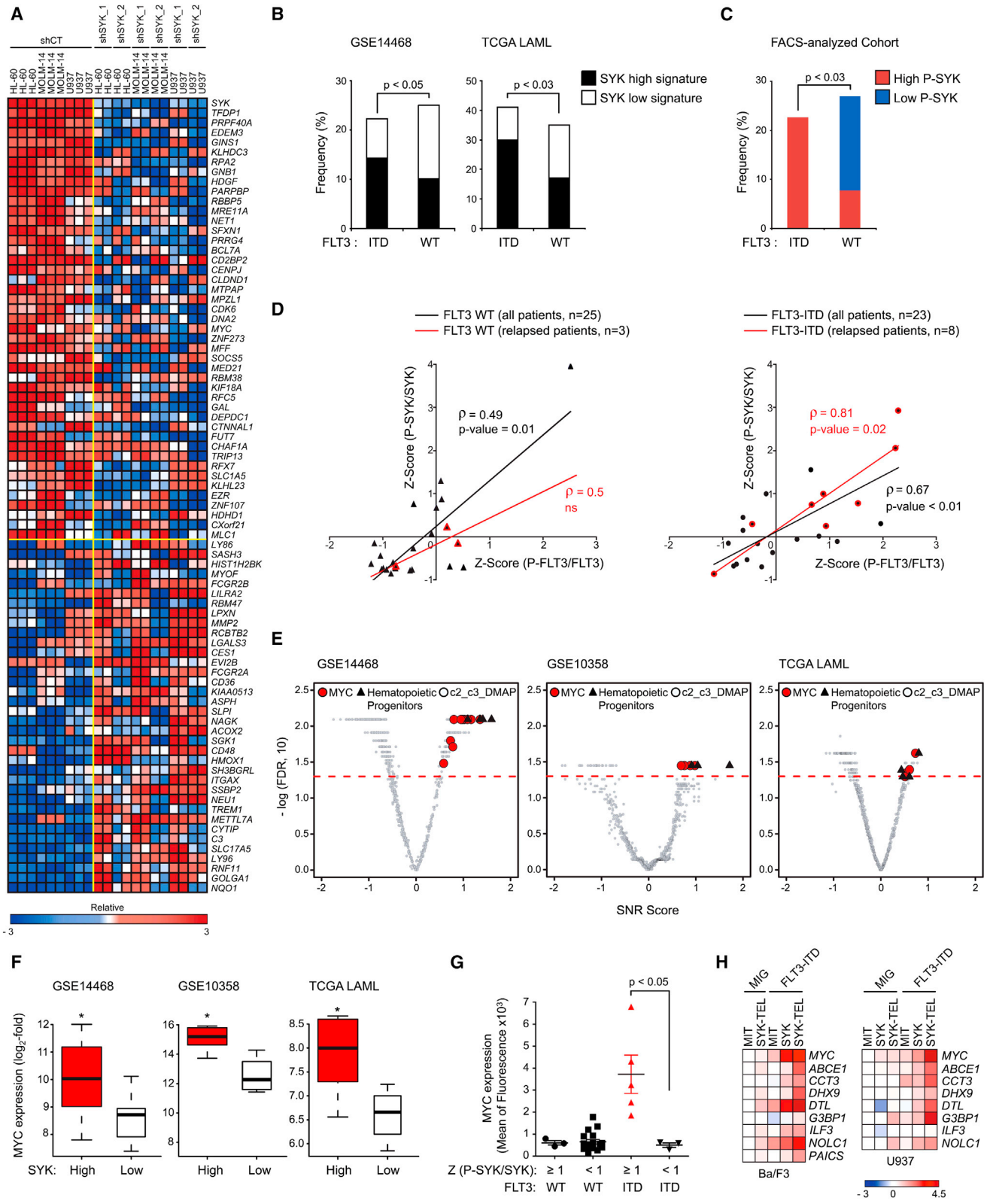

Figure 5. Highly Activated SYK Is Enriched in FLT3-ITD Patient AML Samples and Is Associated with MYC-Related Transcriptional Programs

(A) Heatmap of the top down and upregulated genes following transduction of AML cell lines with CT or two *SYK*-targeting shRNAs based on an SNR score and $p < 0.05$. Data are presented as row normalized.

(legend continued on next page)

S7A–S7D). Finally, H&E staining confirmed that these cells infiltrated the bone marrow and other sites (e.g, liver) (Figure 7B).

We used these secondary transplantable cells to explore the impact of activated SYK on resistance to FLT3 inhibition with the FLT3 inhibitor AC220 (Quizartinib). Although FLT3-ITD-expressing cells were highly sensitive to AC220, those expressing either SYK or SYK-TEL as well as FLT3-ITD showed increased resistance (Figure 7C). This effect was also observed in Ba/F3 cells coexpressing both FLT3-ITD and SYK or SYK-TEL. Interestingly, in vitro and in vivo, these cells were also more resistant to the dual SYK/FLT3 inhibitor, R406, reported to have 5-fold greater potency for SYK than FLT3 (Braselmann et al., 2006) (Figures 7D–7I). AC220 resistance was confirmed in the AML cell lines MOLM-14 and MV4-11 expressing either SYK WT or SYK-TEL and was associated with sustained FLT3 phosphorylation, even in the presence of an otherwise active dose of AC220 (Figures S7E and S7F). Resistance was not observed in vitro with coexpression of FLT3-ITD and the noninteracting partner TEL-SYK, SH2 domain-deleted SYK, KD SYK or SYK-TEL mutants (Figure 7D). These results indicate that the level of SYK activation is correlated with resistance to both molecules and that the physical interaction between SYK and FLT3 is necessary for resistance to the dual inhibitor.

To assess a combination strategy, AC220 and PRT062607 were combined across a range of concentrations and synergy and assessed in vitro using excess over Bliss additive synergy analysis (Figures S7G and S7H). Both compounds synergized to impair the viability of the two cell types as observed by a high excess over Bliss additive. In vivo, in both the SYK WT and SYK-TEL cooperative models with FLT3-ITD, the combination of PRT062607 and AC220 significantly increased survival of mice developing AML (Figures 7E and 7F) and resulted in a marked reduction of leukocytosis, decrease of double GFP/tomato-positive leukemic blasts and profound inhibition of FLT3-ITD and SYK activation (Figures 7G–7I).

DISCUSSION

FLT3-ITD mutations occur in approximately 20% of patients with AML and result in a blockade of differentiation and hyperproliferation of hematopoietic cells (Patel et al., 2012). Early single agent trials were notable for some clinical activity (DeAngelo et al., 2006; Fischer et al., 2010; Knapper et al., 2006; Pratz et al., 2009), but the low complete remission rate as well as the development of progressive disease despite an initial clinical response dampened enthusiasm for using FLT3 inhibitors as a single agent in AML (Weisberg et al., 2010). Newer agents with greater potency and sustained inhibition have been developed with exciting results in recent clinical trials, including the observation of terminal differentiation of AML blasts in patients treated with AC220 (Sexauer et al., 2012). Moreover, mutations within the kinase domain of *FLT3-ITD*, conferring AC220 acquired clinical resistance, were recently reported (Smith et al., 2012), providing additional validation that *FLT3-ITD* is an important oncogenic driver of AML.

In this study, we identify an unexpected functional role for SYK in modulating FLT3 activation and demonstrate FLT3-ITD dependency on SYK for driving myeloid neoplasia in mice despite the constitutive activation of the FLT3 receptor. A role for the SYK-FLT3 collaboration is also highlighted by our in silico and flow-based analysis showing that *FLT3-ITD*-positive patient AML blasts exhibit higher levels of SYK activation than *FLT3*-wild-type patient AML blasts. Although our data reveal the activation of FLT3 by SYK, the mechanism of SYK activation in FLT3-ITD-positive AML remains uncertain. Neither mutation of *SYK* (with the exception of a case report of a *TEL-SYK* rearrangement in a patient with MDS) (Kuno et al., 2001) nor association of SYK activation with other known mutations has previously been described in myeloid neoplasms. Recent manuscripts describe a link between SYK activation and both integrin β2 and β3 signaling (Miller et al., 2013; Oellerich et al., 2013), suggesting two potential mechanisms for SYK activation. Crosstalk between integrin β1 signaling, PYK2, and FLT3-ITD has also been reported (Katsumi et al., 2011), perhaps pointing toward possible feedback of FLT3-ITD on SYK activation.

We engineered a tractable myeloid transplantation model to delineate the effects of various levels of SYK activation on FLT3-ITD-induced disease. This model revealed a link between SYK activation and FLT3-ITD disease progression, with SYK activation leading to acceleration of disease development and transformation from MPD to AML. This is likely dependent on the FLT3-ITD and SYK partnership, rather than exclusively a FLT3-independent effect of SYK, because both the level of SYK activation and the capacity for FLT3 transactivation are essential for the observed effects. The stratification of the FLT3-ITD+ patient group based on high versus low SYK activation highlighted a MYC-driven transcriptional program in the cooperation of SYK with FLT3. In light of this observation, and

(B) Bar graph showing the frequency of primary patient AML samples with *FLT3* WT versus *FLT3-ITD* displaying SYK high versus low signatures in two cohorts GSE14468 (n = 526) and TCGA LAML (n = 179). The p value was calculated using Fisher exact test.
(C) Bar graph showing the frequency of primary patient AML samples with *FLT3* WT (n = 25) versus *FLT3-ITD* (n = 23) exhibiting a high (Z score ≥ 1) versus low (Z score ≤ -1) level of (P-SYK/SYK) evaluated by phospho-flow cytometry on CD13/33-gated population. The p value was calculated using Fisher exact test.
(D) Spearman correlation (ρ-score) between (P-SYK/SYK) and (P-FLT3/FLT3) following Z score normalization across two subgroups of *FLT3* WT and *ITD* patients. Highlighted in red are samples from patients at time of relapse.
(E) Quantitative comparison of gene sets available from the MSig and DMAP database by ssGSEA for patient AML samples with *FLT3-ITD* from three different cohorts (GSE 14468, 10358, and TCGA LAML) displaying a SYK high versus low signature. Red dots indicate sets for *MYC*, black triangles for hematopoietic progenitors, and gray for all other available gene sets.
(F) Comparison of MYC expression levels for patient samples with *FLT3-ITD* from three different cohorts (GSE 14468, 10358, and TCGA LAML) displaying a SYK high versus low signature. The p value was calculated using Fisher exact test. Error bars represent mean ± SD.
(G) MYC protein level evaluated by intracellular flow cytometry on a cohort of *FLT3* WT or *ITD* patient samples (n = 25) exhibiting either high (Z score [P-SYK/SYK] ≥ 1) or medium to low (Z score [P-SYK/SYK] < 1) SYK activation. The p value was calculated using a Mann-Whitney test. Error bars represent mean ± SEM.
(H) Heatmap showing expression level of MYC transcriptional target genes evaluated by qRT-PCR. Normalized data are presented as a $\log_2$-ratio versus MIT.
See also Figure S5 and Tables S1, S2, and S3.

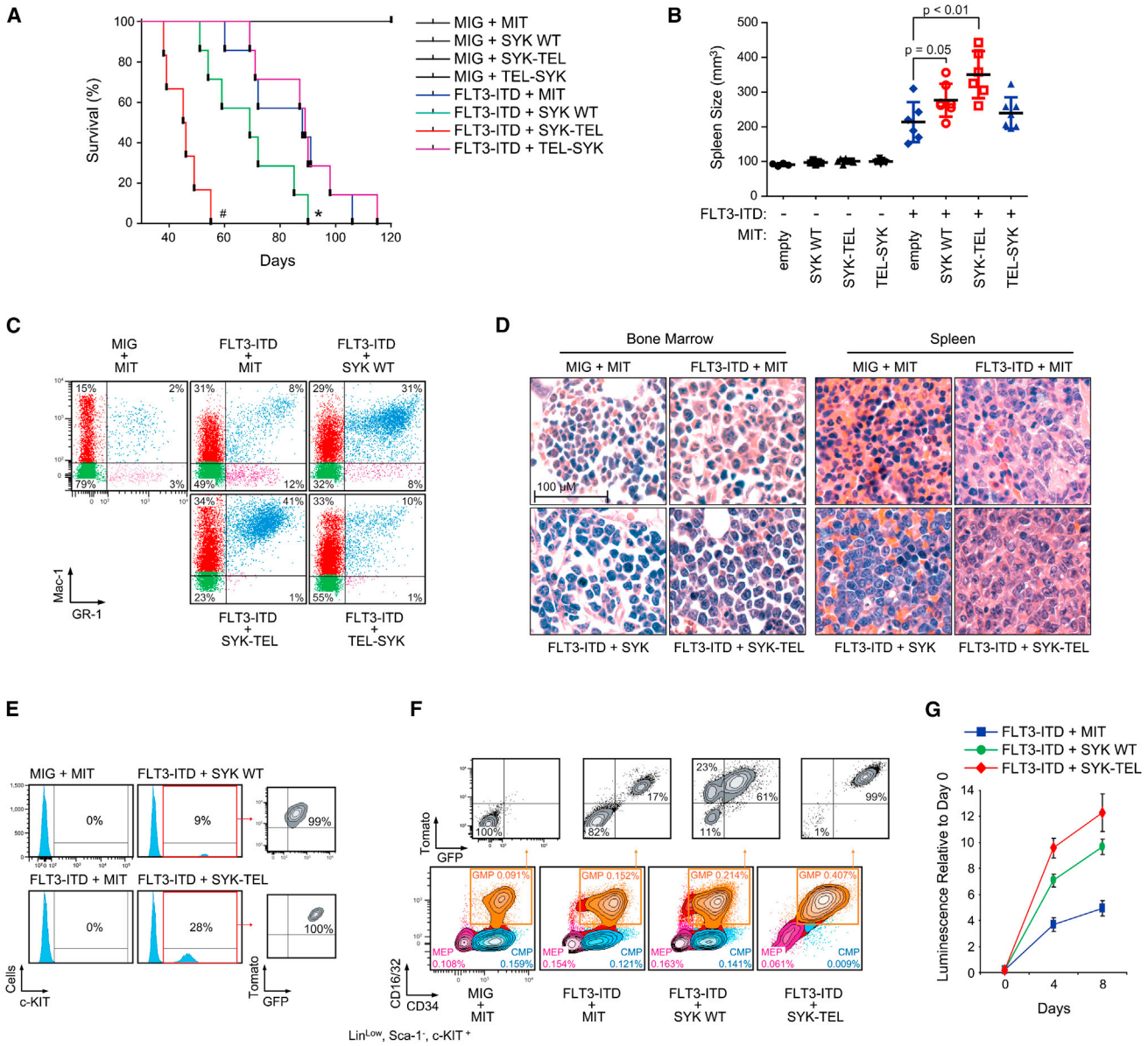

(legend on next page)

because the overexpression of this transcription factor has the capacity to induce AML (Luo et al., 2005), MYC has been nominated as one candidate for explaining the mechanism for the transition from MPD to an AML-like disease emerging from the SYK-FLT3 synergistic signal.

Our study has important clinical implications. First, we identify an increased sensitivity to SYK inhibition in the specific FLT3-ITD-positive AML subtype, suggesting the testing of SYK inhibitors in this patient population. We also identified a strong positive correlation between SYK and FLT3 activation in a subgroup of relapsed FLT3-ITD patient samples, nominating the SYK/FLT3-ITD cooperation as a potential mechanism of chemoresistance and inviting further study of the relationship between SYK activation and prognosis in FLT3 mutated AML. Moreover, our study reveals that the secondary transplantable AML, driven by the coexpression of highly activated SYK and FLT3-ITD, exhibits moderate resistance to the single FLT3 inhibitor AC220 and strong resistance to the dual SYK/FLT3 inhibitor fostamatinib (R406). Among the possible mechanisms to explain this surprising resistance to fostamatinib are inadequate pharmacokinetics with a failure to sufficiently inhibit SYK and FLT3 or an altered binding/inhibiting capacity of the compound due to the physical association between SYK and FLT3. A similar observation has been made in CML where another tyrosine kinase, LYN, can cooperate with BCR-ABL to overcome BCR-ABL small-molecule inhibition by mediating BCR-ABL phosphorylation even in the presence of inhibitor (Wu et al., 2008). The finding that the SYK mutant lacking the ability to transactivate FLT3 failed to promote resistance supports a similar mechanism of action for SYK-mediated FLT3 resistance. In this context, whereas SYK or FLT3 inhibition alone had some activity in vivo, the combined treatment with the SYK and FLT3 specific inhibitors was highly efficacious, suggesting this combination for clinical testing.

In summary, we report that the level of SYK activation is critical for outcome in mice developing a FLT3-ITD-driven myeloid neoplasia, illustrating the notion that additional interacting partners are essential in the oncogenic effects of FLT3 in promoting disease. This study also reveals the important clinical translational finding that *FLT3-ITD* AML cells have increased sensitivity to SYK suppression, raises the possibility that SYK hyperactivation may attenuate the response to FLT3 inhibitors, and supports the testing of FLT3 inhibitors in combination with SYK inhibitors in patients with FLT3 mutant AML.

EXPERIMENTAL PROCEDURES

See Supplemental Experimental Procedures for detailed methods.

High-Throughput Kinase Activity Profiling

A Luminex immunosandwich assay was performed in AML cells stably transduced with a pWZL empty or *SYK-TEL* vector encoding for a constitutively activated form of SYK. One hundred micrograms of whole-cell lysates from each cell line and positive control lysates were quantified, and equal concentrations of protein were incubated with a mixture of antibody-coupled Luminex beads directed against 105 protein candidates and then with a secondary anti-phospho-tyrosine biotin-labeled 4G10 antibody (Millipore).

Growth Measurement

Cells were plated in 384-well plates. ATP content was measured using CellTiter Glo (Promega) per the manufacturer's instructions.

Flow-Based Myeloid Differentiation Screening

U937, MOLM-14, THP-1, and KBM-3 cells were arrayed in two series of three replicates per shRNA in round bottom 96-well tissue culture plates. The next day, cells were infected, incubated for 5 days, and stained. Heatmap projections on differentially expressed CD11b and CD14 across each hairpin-transduced cell line were created based on the GENE-E software (http://www.broadinstitute.org/cancer/software/GENE-E/).

In Vivo Transplantation

The Massachusetts Institute of Technology Committee on Animal Care reviewed and approved all mouse experiments. The 4-week-old BALB/c male donor mice were primed with an intraperitoneal injection of 5′-fluorouracil (150 mg/kg) and sacrificed after 6 days. Bone marrow was harvested from the femur, tibia, and humerus, and red blood cells were lysed (RBCL buffer, Sigma). Myeloid cells were sorted and infected with the different combination of vectors and reinjected into recipient irradiated mice.

Figure 6. High SYK Activation Synergizes with FLT3-ITD to Promote Progression to AML

(A) Kaplan-Meier curves showing overall survival of mice (n = 7 for each group except for *FLT3-ITD* + *SYK-TEL* group, for which n = 6) transplanted with myeloid cells expressing each combination of indicated constructs. Statistical significance determined by log-rank (Mantel-Cox) test. *p = 0.05 and #p < 0.01 by comparison with *FLT3-ITD* + MIT group.

(B) Spleen size measurement by microtomography of six mice per group when *FLT3-ITD* + *SYK-TEL* mice became moribund. The p value was calculated using a Mann-Whitney test. Error bars represent mean ± SEM.

(C) FACS analysis of Mac-1 and GR-1 expressing populations in spleen. A representative FACS plot from each group is shown. Analysis was performed after *FLT3-ITD* + *SYK-TEL* mice became moribund.

(D) H&E staining of bone marrow and spleen of a representative moribund mouse from each indicated group.

(E) FACS analysis of *c-KIT* expressing cells in spleen after 5 days in culture. One representative moribund mouse from each indicated group is shown.

(F) Proportion of CMP (CD16/32$^-$/CD34$^+$), GMP (CD16/32$^+$/CD34$^+$), and MEP (CD16/32$^-$/CD34$^-$) cell populations on gated Lin^{Low}/Sca-1$^-$/c-KIT$^+$ myeloid progenitors. Tomato and GFP expression were evaluated on each GMP cell population. One representative moribund mouse from each group is shown.

(G) Double tomato and GFP positive Lin^{Low}/Sca-1$^-$/c-KIT$^+$ myeloid cells were sorted from the whole bone marrow harvested from moribund mice transplanted with each combination of *FLT3-ITD* and *SYK* vectors. Growth after sorting is shown relative to the day 0 (time of seeding) values, with error bars representing the mean ± SD.

(H and I) Purified normal CD34$^+$ human primary cells were infected with *FLT3-ITD* in combination with different forms of *SYK* (wild-type, constitutively active *SYK-TEL*, or inactive *SYK-TEL* KD) (H) or *SYK-TEL* in combination with either *FLT3-ITD* or the two mutants *FLT3-ITD* Y768A and Y955A (I). Colony number was evaluated after MTT staining. $p < 0.01$ and $p < 0.05$, calculated using a Mann-Whitney test. Error bars represent mean ± SD.

(J) Kaplan-Meier curves showing overall survival of mice (n = 5 for each group) transplanted with myeloid cells expressing each indicated combination of *FLT3-ITD* or *FLT3-ITD* mutants (Y > A) in combination with *SYK-TEL*. Statistical significance determined by log-rank (Mantel-Cox) test. *p = 0.05 by comparison with *FLT3-ITD* group.

See also Figure S6.

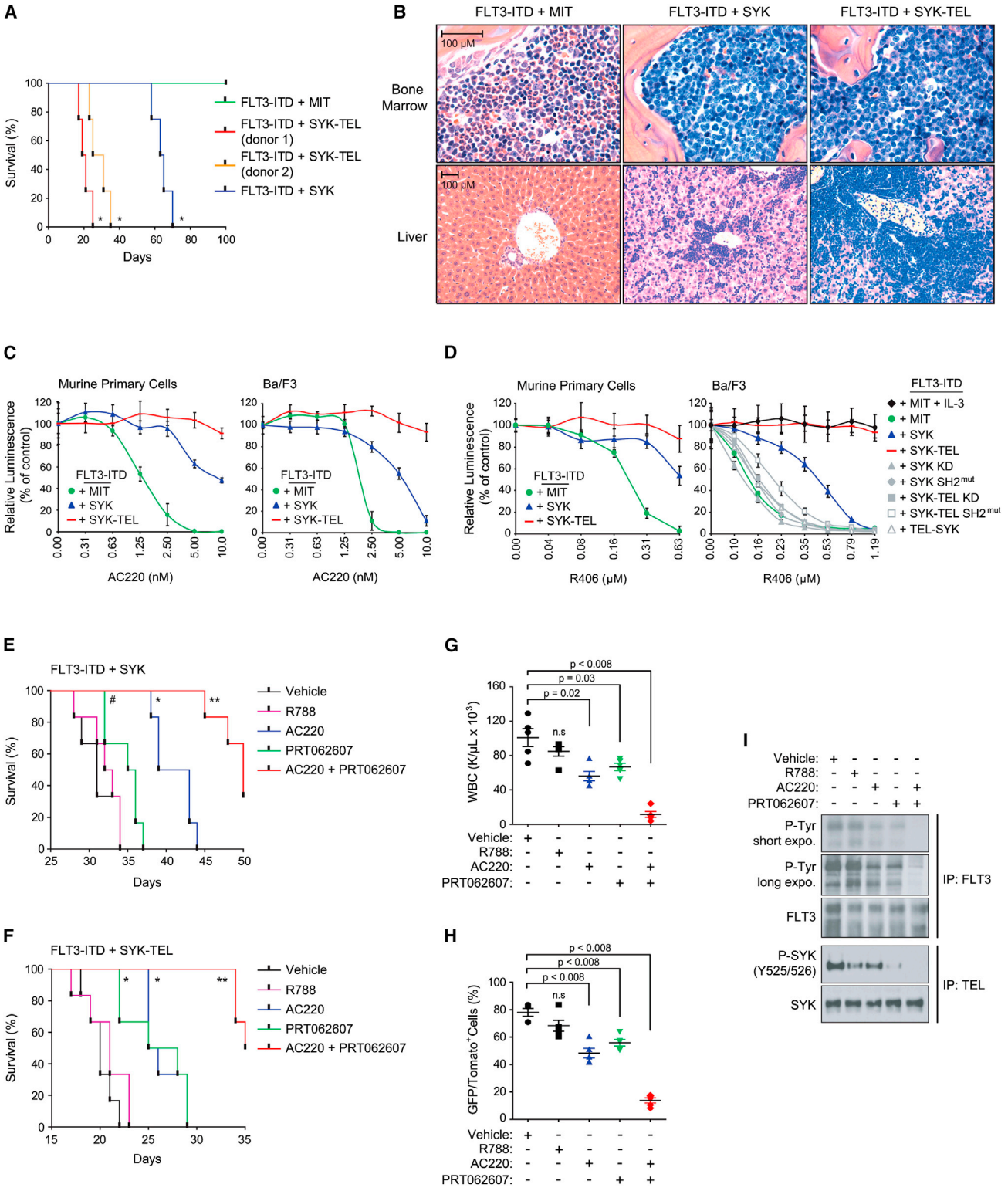

Figure 7. High SYK Activation Impairs the Targeting of FLT3-ITD-Driven AML with Small-Molecule Inhibitors In Vitro and In Vivo

(A) Kaplan-Meier curves showing overall survival of mice (n = 4) secondary transplanted with double tomato and GFP-positive myeloid cells expressing *FLT3-ITD* in combination with MIT empty, *SYK* WT, or *SYK-TEL* (clones from two different donor mice). Statistical significance determined by log-rank (Mantel-Cox) test.

(B) H&E staining of the bone marrow and liver of a representative moribund mouse from each indicated group.

(C and D) Growth inhibition of secondary transplantable murine primary and Ba/F3 cells coexpressing *FLT3-ITD* and indicated *SYK* constructs and treated with increasing doses of either AC220 (C) or R406 (D). Values are shown relative to day 0 (time of seeding), with error bars representing the mean ± SD.

(legend continued on next page)

Primary Cell Studies

Normal purified $CD34^+$ human cells were obtained from Lonza. Use of these materials is considered exempt as Human Subjects by the Dana-Farber Cancer Institute Internal Review Board. Primary patient AML blasts were collected after obtaining patient informed consent under Dana-Farber Cancer Institute Internal Review Board-approved protocols.

ACCESSION NUMBERS

The Gene Expression Omnibus (GEO) accession number for the genome-wide expression analysis reported in this paper is GSE54065.

SUPPLEMENTAL INFORMATION

Supplemental Information includes Supplemental Experimental Procedures, seven figures, and three tables and can be found with this article online at http://dx.doi.org/10.1016/j.ccr.2014.01.022.

ACKNOWLEDGMENTS

We thank Merck for providing their small-molecule inhibitor of SYK. This research was supported by grants from the National Cancer Institute (R01 CA140292), the American Cancer Society, the Starr Cancer Consortium, Project Cupid and One Mission (to K.S.), and the Swedish Research Council and Swedish Cancer Society (to L.R. and J.U.K.). A.P. is a Leukemia and Lymphoma Society (LLS) Fellow, and K.S. is an LLS Scholar.

Received: April 24, 2013
Revised: November 14, 2013
Accepted: January 22, 2014
Published: February 10, 2014

REFERENCES

Bernt, K.M., Zhu, N., Sinha, A.U., Vempati, S., Faber, J., Krivtsov, A.V., Feng, Z., Punt, N., Daigle, A., Bullinger, L., et al. (2011). MLL-rearranged leukemia is dependent on aberrant H3K79 methylation by DOT1L. Cancer Cell *20*, 66–78.

Braselmann, S., Taylor, V., Zhao, H., Wang, S., Sylvain, C., Baluom, M., Qu, K., Herlaar, E., Lau, A., Young, C., et al. (2006). R406, an orally available spleen tyrosine kinase inhibitor blocks fc receptor signaling and reduces immune complex-mediated inflammation. J. Pharmacol. Exp. Ther. *319*, 998–1008.

Daigle, S.R., Olhava, E.J., Therkelsen, C.A., Majer, C.R., Sneeringer, C.J., Song, J., Johnston, L.D., Scott, M.P., Smith, J.J., Xiao, Y., et al. (2011). Selective killing of mixed lineage leukemia cells by a potent small-molecule DOT1L inhibitor. Cancer Cell *20*, 53–65.

DeAngelo, D.J., Stone, R.M., Heaney, M.L., Nimer, S.D., Paquette, R.L., Klisovic, R.B., Caligiuri, M.A., Cooper, M.R., Lecerf, J.M., Karol, M.D., et al. (2006). Phase 1 clinical results with tandutinib (MLN518), a novel FLT3 antagonist, in patients with acute myelogenous leukemia or high-risk myelodysplastic syndrome: safety, pharmacokinetics, and pharmacodynamics. Blood *108*, 3674–3681.

Deshpande, A.J., Bradner, J., and Armstrong, S.A. (2012). Chromatin modifications as therapeutic targets in MLL-rearranged leukemia. Trends Immunol. *33*, 563–570.

Fischer, T., Stone, R.M., Deangelo, D.J., Galinsky, I., Estey, E., Lanza, C., Fox, E., Ehninger, G., Feldman, E.J., Schiller, G.J., et al. (2010). Phase IIB trial of oral Midostaurin (PKC412), the FMS-like tyrosine kinase 3 receptor (FLT3) and multi-targeted kinase inhibitor, in patients with acute myeloid leukemia and high-risk myelodysplastic syndrome with either wild-type or mutated FLT3. J. Clin. Oncol. *28*, 4339–4345.

Friedberg, J.W., Sharman, J., Sweetenham, J., Johnston, P.B., Vose, J.M., Lacasce, A., Schaefer-Cutillo, J., De Vos, S., Sinha, R., Leonard, J.P., et al. (2010). Inhibition of Syk with fostamatinib disodium has significant clinical activity in non-Hodgkin lymphoma and chronic lymphocytic leukemia. Blood *115*, 2578–2585.

Griffith, J., Black, J., Faerman, C., Swenson, L., Wynn, M., Lu, F., Lippke, J., and Saxena, K. (2004). The structural basis for autoinhibition of FLT3 by the juxtamembrane domain. Mol. Cell *13*, 169–178.

Hahn, C.K., Berchuck, J.E., Ross, K.N., Kakoza, R.M., Clauser, K., Schinzel, A.C., Ross, L., Galinsky, I., Davis, T.N., Silver, S.J., et al. (2009). Proteomic and genetic approaches identify Syk as an AML target. Cancer Cell *16*, 281–294.

Katsumi, A., Kiyoi, H., Abe, A., Tanizaki, R., Iwasaki, T., Kobayashi, M., Matsushita, T., Kaibuchi, K., Senga, T., Kojima, T., et al. (2011). FLT3/ITD regulates leukaemia cell adhesion through $\alpha4\beta1$ integrin and Pyk2 signalling. Eur. J. Haematol. *86*, 191–198.

Keshvara, L.M., Isaacson, C., Harrison, M.L., and Geahlen, R.L. (1997). Syk activation and dissociation from the B-cell antigen receptor is mediated by phosphorylation of tyrosine 130. J. Biol. Chem. *272*, 10377–10381.

Knapper, S., Burnett, A.K., Littlewood, T., Kell, W.J., Agrawal, S., Chopra, R., Clark, R., Levis, M.J., and Small, D. (2006). A phase 2 trial of the FLT3 inhibitor lestaurtinib (CEP701) as first-line treatment for older patients with acute myeloid leukemia not considered fit for intensive chemotherapy. Blood *108*, 3262–3270.

Kuno, Y., Abe, A., Emi, N., Iida, M., Yokozawa, T., Towatari, M., Tanimoto, M., and Saito, H. (2001). Constitutive kinase activation of the TEL-Syk fusion gene in myelodysplastic syndrome with t(9;12)(q22;p12). Blood *97*, 1050–1055.

Ley, T., Miller, C., Ding, L., Raphael, B., Mungall, A., Robertson, A., Hoadley, K., Triche, T.J., Laird, P., Baty, J., et al.; Cancer Genome Atlas Research Network (2013). Genomic and epigenomic landscapes of adult de novo acute myeloid leukemia. N. Engl. J. Med. *368*, 2059–2074.

Luo, H., Li, Q., O'Neal, J., Kreisel, F., Le Beau, M.M., and Tomasson, M.H. (2005). c-Myc rapidly induces acute myeloid leukemia in mice without evidence of lymphoma-associated antiapoptotic mutations. Blood *106*, 2452–2461.

Miller, P.G., Al-Shahrour, F., Hartwell, K.A., Chu, L.P., Järås, M., Puram, R.V., Puissant, A., Callahan, K.P., Ashton, J., McConkey, M.E., et al. (2013). In Vivo RNAi screening identifies a leukemia-specific dependence on integrin beta 3 signaling. Cancer Cell *24*, 45–58.

Mócsai, A., Ruland, J., and Tybulewicz, V.L. (2010). The SYK tyrosine kinase: a crucial player in diverse biological functions. Nat. Rev. Immunol. *10*, 387–402.

Moon, K.D., Post, C.B., Durden, D.L., Zhou, Q., De, P., Harrison, M.L., and Geahlen, R.L. (2005). Molecular basis for a direct interaction between the Syk protein-tyrosine kinase and phosphoinositide 3-kinase. J. Biol. Chem. *280*, 1543–1551.

Moy, L.Y., Jia, Y., Caniga, M., Lieber, G., Gil, M., Fernandez, X., Sirkowski, E., Miller, R., Alexander, J.P., Lee, H.H., et al. (2013). Inhibition of spleen tyrosine

(E and F) Kaplan-Meier curves showing overall survival of mice (n = 6) secondary transplanted with double tomato and GFP positive myeloid cells expressing *FLT3-ITD* in combination with *SYK* WT (E), or *SYK-TEL* (F) and treated with vehicle, R788 (R406 prodrug, Fostamatinib), PRT062607, AC220, or a combination of PRT062607 + AC220. Statistical significance determined by log-rank (Mantel-Cox) test. $^{\#}p < 0.02$, $^{*}p < 0.002$, and $^{**}p \leq 0.0008$ by comparison with vehicle-treated group.

(G and H) WBC count in the blood harvested from five mice per group at day 10 posttreatment (G). Proportion of double tomato and GFP positive secondary transplanted *FLT3-ITD* + *SYK-TEL* cells in spleen of five mice sacrificed at day 15 posttreatment (H). The p value was calculated using a Mann-Whitney test in comparison with vehicle condition. n.s, nonsignificant ($p > 0.05$). Error bars represent mean ± SEM.

(I) Western blot showing the levels of FLT3 and SYK phosphorylation on *FLT3-ITD* + *SYK-TEL* cells sorted from spleen of mice treated for 3 days with indicated compounds.

See also Figure S7.

kinase attenuates allergen-mediated airway constriction. Am. J. Respir. Cell Mol. Biol. *49*, 1085–1092.

Oellerich, T., Oellerich, M.F., Engelke, M., Munch, S., Mohr, S., Nimz, M., Hsiao, H.H., Corso, J., Zhang, J., Bohnenberger, H., et al. (2013). β_2 integrin-derived signals induce cell survival and proliferation of AML blasts by activating a Syk/STAT signaling axis. Blood *121*, 3889–3899.

Patel, J.P., Gönen, M., Figueroa, M.E., Fernandez, H., Sun, Z., Racevskis, J., Van Vlierberghe, P., Dolgalev, I., Thomas, S., Aminova, O., et al. (2012). Prognostic relevance of integrated genetic profiling in acute myeloid leukemia. N. Engl. J. Med. *366*, 1079–1089.

Pechloff, K., Holch, J., Ferch, U., Schweneker, M., Brunner, K., Kremer, M., Sparwasser, T., Quintanilla-Martinez, L., Zimber-Strobl, U., Streubel, B., et al. (2010). The fusion kinase ITK-SYK mimics a T cell receptor signal and drives oncogenesis in conditional mouse models of peripheral T cell lymphoma. J. Exp. Med. *207*, 1031–1044.

Pratz, K.W., Cortes, J., Roboz, G.J., Rao, N., Arowojolu, O., Stine, A., Shiotsu, Y., Shudo, A., Akinaga, S., Small, D., et al. (2009). A pharmacodynamic study of the FLT3 inhibitor KW-2449 yields insight into the basis for clinical response. Blood *113*, 3938–3946.

Sexauer, A., Perl, A., Yang, X., Borowitz, M., Gocke, C., Rajkhowa, T., Thiede, C., Frattini, M., Nybakken, G.E., Pratz, K., et al. (2012). Terminal myeloid differentiation in vivo is induced by FLT3 inhibition in FLT3/ITD AML. Blood *120*, 4205–4214.

Smith, C.C., Wang, Q., Chin, C.S., Salerno, S., Damon, L.E., Levis, M.J., Perl, A.E., Travers, K.J., Wang, S., Hunt, J.P., et al. (2012). Validation of ITD mutations in FLT3 as a therapeutic target in human acute myeloid leukaemia. Nature *485*, 260–263.

Spurgeon, S.E., Coffey, G., Fletcher, L.B., Burke, R., Tyner, J.W., Druker, B.J., Betz, A., DeGuzman, F., Pak, Y., Baker, D., et al. (2013). The selective SYK inhibitor P505-15 (PRT062607) inhibits B cell signaling and function in vitro and in vivo and augments the activity of fludarabine in chronic lymphocytic leukemia. J. Pharmacol. Exp. Ther. *344*, 378–387.

Swords, R., Freeman, C., and Giles, F. (2012). Targeting the FMS-like tyrosine kinase 3 in acute myeloid leukemia. Leukemia *26*, 2176–2185.

Umehara, H., Huang, J.Y., Kono, T., Tabassam, F.H., Okazaki, T., Gouda, S., Nagano, Y., Bloom, E.T., and Domae, N. (1998). Co-stimulation of T cells with CD2 augments TCR-CD3-mediated activation of protein tyrosine kinase p72syk, resulting in increased tyrosine phosphorylation of adapter proteins, Shc and Cbl. Int. Immunol. *10*, 833–845.

Weisberg, E., Sattler, M., Ray, A., and Griffin, J.D. (2010). Drug resistance in mutant FLT3-positive AML. Oncogene *29*, 5120–5134.

Williams, R.T., Roussel, M.F., and Sherr, C.J. (2006). Arf gene loss enhances oncogenicity and limits imatinib response in mouse models of Bcr-Abl-induced acute lymphoblastic leukemia. Proc. Natl. Acad. Sci. USA *103*, 6688–6693.

Wu, J., Meng, F., Lu, H., Kong, L., Bornmann, W., Peng, Z., Talpaz, M., and Donato, N.J. (2008). Lyn regulates BCR-ABL and Gab2 tyrosine phosphorylation and c-Cbl protein stability in imatinib-resistant chronic myelogenous leukemia cells. Blood *111*, 3821–3829.

Zuber, J., Shi, J., Wang, E., Rappaport, A.R., Herrmann, H., Sison, E.A., Magoon, D., Qi, J., Blatt, K., Wunderlich, M., et al. (2011). RNAi screen identifies Brd4 as a therapeutic target in acute myeloid leukaemia. Nature *478*, 524–528.